JOC Article

Mechanisms of Staudinger Reactions within Density Functional Theory

Wei Quan Tian and Yan Alexander Wang*

Department of Chemistry, University of British Columbia, Vancouver BC V6T 1Z1, Canada

yawang@chem.ubc.ca

Received February 21, 2004

The Staudinger reactions of substituted phosphanes and azides have been investigated by using density functional theory. Four different initial reaction mechanisms have been found. All systems studied go through a *cis*-transition state rather than a *trans*-transition state or a one-step transition state. The one-step pathway of the phosphorus atom attacking the substituted nitrogen atom is always unfavorable energetically. Depending on the substituents on the azide and the phosphane, the reaction mechanism with the lowest initial reaction barrier can be classified into three categories: (1) like the parent reaction, $PH_3 + N_3H$, the reaction goes through a *cis*-transition state, approaches a *cis*-intermediate, overcomes a PN-bond-shifting transition state, reaches a four-membered ring intermediate, dissociates N_2 by overcoming a small barrier, and results in the final products: N_2 and a phosphazene; (2) once reaching the *cis*-intermediate, the reaction goes through the N_2-eliminating transition state and produces the final products; (3) the reaction has a concerted initial *cis*-transition state, in which the phosphorus atom attacks the first and the third nitrogen atoms of the azide simultaneously and reaches an intermediate, and then the reaction goes through similar steps of the first reaction mechanism. In contrast to the previous predictions on the relative stability of the unsubstituted *cis*-configured phosphazide intermediate and the unsubstituted *trans*-configured phosphazide intermediate, the total energy of the substituted *trans*-configured phosphazide intermediate is close to that of the substituted *cis*-configured phosphazide intermediate. The preference of the initial *cis*-transition state reaction pathway is thoroughly discussed. The relative stability of the *cis*- and the *trans*-intermediates is explored and analyzed with the aid of molecular orbitals. The effects of substituents and solvent effects on the reaction mechanisms of the Staudinger reactions are discussed in detail.

I. Introduction

Phosphorus chemistry plays important roles in catalysis[1], polymer science[2], biological engineering[3], synthetic chemistry,[4] and life.[5]

The Staudinger reaction,[6] involving phosphanes (**A**) reacting with azides (**B**)[2] to form phosphazenes (**C**) and nitrogen molecules (Scheme 1), was recently utilized as a measure of chemical control over complex biological systems[3a] and was regarded as a new possibility for probing intercellular interactions[3b].

SCHEME 1

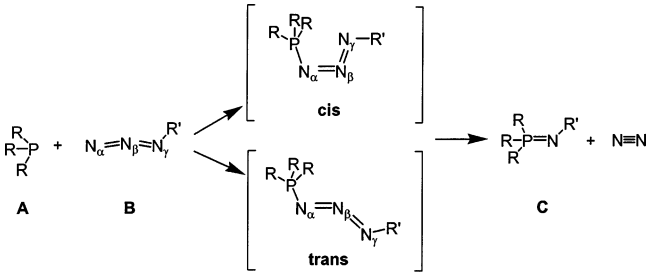

This reaction has been recognized as a useful reaction in organic chemistry[5−13] and biology.[3,13] According to an

(1) (a) Stephan, D. W. *Angew. Chem., Int. Ed.* **2000**, *39*, 314. (b) Hollink, E.; Stewart, J. C.; Wei, P.; Stephan, D. W. *Dalton Trans.* **2003**, 3968. (c) Yue, N.; Hollink, E.; Guérin, F.; Stephan, D. W. *Organometallics* **2001**, *20*, 4424. (d) Stephan, D. W.; Guérin, F.; Spence, R. E. v.; Koch, L.; Gao, X.; Brown, S. J.; Swabey, J. W.; Wang, Q.; Xu, W.; Zoricak, P.; Harrison, D. G. *Organometallics* **1999**, *18*, 2046.

(2) (a) Wright, V. A.; Gates, D. P. *Angew. Chem., Int. Ed.* **2002**, *41*, 2389. (b) Tang, C.-W.; Yam, M.; Gates, D. P. *J. Am. Chem. Soc.* **2003**, *125*, 1480. (c) Allcock, H. R. *Chemistry and Applications of Polyphosphazenes*; Wiley: New Jersey, 2003.

(3) (a) Saxon, E.; Luchansky, S. J.; Hang, H. C.; Yu, C.; Lee, S. C.; Bertozzi, C. R. *J. Am. Chem. Soc.* **2002**, *124*, 14893. (b) Saxon, E.; Bertozzi, C. R. *Science* **2000**, *287*, 2007.

(4) (a) Majoral, J.-P.; Caminade, A.-M.; Maraval, V. *Chem. Commun.* **2002**, 2929. (b) LePichon, L.; Stephan, D. W. *Inorg. Chem.* **2001**, *40*, 3827. (c) Bieger, K.; Bouhadir, G.; Réau, R.; Dahan, F.; Bertrand, G. *J. Am. Chem. Soc.* **1996**, *118*, 1038.

(5) (a) Cordridge, D. E. C. *Phosphorus 2000: Chemistry, Biochemistry & Technology*; Elsevier: Amsterdam, 2000. (b) Irving, J. T. *Calcium and Phosphorus Metabolism*; Academic Press: New York, 1973.

(6) Staudinger, H.; Meyer, J. *Helv. Chim. Acta* **1919**, *2*, 635.

(7) Gololobov, Yu. G.; Zhmurova, I. N.; Kasukhin, L. F. *Tetrahedron* **1981**, *37*, 437.

(8) Gololobov, Yu. G.; Zhmurova, I. N.; Kasukhin, L. F. *Tetrahedron* **1992**, *48*, 1353.

(9) Molina, P.; Arques, A.; Vinader, M. V. *J. Org. Chem.* **1990**, *55*, 4724.

(10) Tang, J.; Dopke, J.; Verkade, J. G. *J. Am. Chem. Soc.* **1993**, *115*, 5015.

(11) Shalev, D. E.; Chiacchiera, S. M.; Radkowsky, A. E.; Kosower, E. M. *J. Org. Chem.* **1996**, *61*, 1689.

10.1021/jo049702n CCC: $27.50
Published on Web 06/02/2004

observation of the kinetics of a trapping experiment,[14] the Staudinger reaction of phenyl azides and triphenylphosphanes goes through two transition states with one yellow or orange intermediate complex. It was further proposed that the phosphane attacks the external nitrogen atom N_α (no substituent on this nitrogen atom) of the azide from a preferred direction for the initial reaction.[14] X-ray diffraction studies also supported the proposal for the existence of intermediate complexes in the Staudinger reaction.[15−20] The intermediate complexes have been further characterized by NMR,[21] UV−vis,[21b] and the Raman spectra.[22]

As a result of the relative conformation of the $PN_\alpha N_\beta N_\gamma$ unit in the intermediate complexes, two possible conformations emerge, *cis* and *trans*. (It has been well established both experimentally and theoretically that the $N_\alpha N_\beta N_\gamma$ backbone of an azide is not linear; the A_{NNN} angle is about 170°. See ref 39 for more details.) In the *cis*-conformation, the phosphorus atom and the end nitrogen atom N_γ (with substituent on this nitrogen atom) are on the same side of the central $N_\alpha N_\beta$ bond, whereas they are at different sides of the central $N_\alpha N_\beta$ bond in the *trans*-conformation. Both the *cis*-intermediate[15,18−20] and the *trans*-intermediate[16,17] have been observed experimentally. However, the complete reaction mechanism of the Staudinger reaction remains unclear.

Theoretical chemistry becomes indispensable in uncovering reaction mechanisms and developing new materials; the progress of computational chemistry certainly accelerates the progress in chemistry,[23] life science,[24] and materials science.[25] Thorough understanding of a reaction mechanism helps to control chemical reactions and develop new materials. Only recently has the reaction profile of the Staudinger reaction for the model system ($PH_3 + N_3H$) been studied with quantum chemical methods.[20,26] At the CCSD(T)/6-31G(d,p)[27,28] level with a MP2(full)/6-31G(d)[28,29] optimized geometry, Widauer and co-workers[20] explored the main reaction pathway for the Staudinger reaction of $PH_3 + N_3H$ starting from a *trans*-intermediate.[18] In this work, the *cis*-intermediate was found to be more stable than the *trans*-intermediate, which contradicts an earlier prediction[18] using the Hartree−Fock (HF) method. The N_2-dissociation region on the potential energy surface was also found to be very flat;[20] the energy of the last intermediate was predicted to be lower than the energy of the N_2-dissociation transition state after the zero point vibrational energy (ZPVE) correction. However, Widauer and co-workers[20] did not study the stationary points on the potential energy surface for the initial reaction of $PH_3 + N_3H$.

In another computational investigation,[26] the complete reaction profile was studied at the level of HF/6-31G(d). The initial *trans*-transition state has not been located by the hybrid density functional theory (DFT)-based method B3LYP.[30,31] It was found that the *cis*-intermediate can easily isomerize to the *trans*-intermediate. The *cis*-intermediate can also readily isomerize to a cyclic intermediate, which in turn eliminates the N_2 molecule almost without reaction barrier, because the potential energy surface is very flat around this region.[26] The relative stability of the *cis*-intermediate and the *trans*-intermediate was rationalized according to the interaction between orbital interactions in natural bond orbital (NBO) analysis.[26] The proposed explanation of the relative stability of the *cis*- and the *trans*-intermediates does not seem to be able to account for the experimental observations of both *cis*- and *trans*-intermediates.[17−19]

Though the substitution effects have been investigated theoretically, only one substituent on P and one substituent on N_γ were studied to date.[26] The reason PH_3 prefers to attack N_3H from the *cis* direction has not been computationally investigated thus far.[20,26]

Besides the external N_α attack, the Staudinger reaction could also possibly occur upon the phosphane's attack on the substituted nitrogen N_γ. If this does happen, will it go through a one-step transition state or multiple steps to finalize the reaction? This mechanism was never proposed or investigated computationally.

We have carried out DFT[32]-based calculations to better understand the reaction mechanisms of the Staudinger reactions, the preference of reaction pathway for the

(12) Taillefer, M.; Inguimbert, N.; Jäger, L.; Merzweiler, K.; Cristau, H.-J. *Chem. Commun.* **1999**, 565.
(13) Kato, H.; Ohmori, K.; Suzuki, K. *Synlett* **2001**, *SI*, 1003.
(14) Leffler, J. E.; Temple, R. D. *J. Am. Chem. Soc.* **1967**, *89*, 5235.
(15) (a) Hillhouse, G. L.; Goeden, G. V.; Haymore, B. L. *Inorg. Chem.* **1982**, *21*, 2064. (b) Hillhouse, G. L.; Haymore, B. L. *J. Organomet. Chem.* **1978**, *162*, C23
(16) Buschmann, R. R.; Luger, P.; Gregson, D.; Trummlitz, G. *Acta Crystallogr.* **1988**, *C44*, 1083.
(17) Goerlich, R.; Farkens, M.; Fischer, A.; Jones, P. G.; Schmutzler, R. *Z. Anorg. Allg. Chem.* **1994**, *620*, 707.
(18) Molina, P.; López-Leonardo, C.; Llamas-Botía, J.; Foces-Foces, C.; Fernández-Castaño, C. *Tetrahedron* **1996**, *52*, 9629.
(19) Alajarín, M.; Molina, P.; López-Leonardo, C. *Angew. Chem., Int. Ed. Engl.* **1997**, *36*, 67.
(20) Widauer, C.; Grützmacher, H.; Shevchenko, I.; Gramlich, V. *Eur. J. Inorg. Chem.* **1999**, 1659.
(21) (a) Velasco, D. M.; Molina, P.; Freaneda, P. M.; Sanz, M. A. *Tetrahedron* **2000**, *56*, 4079. (b) Goldwhite, H.; Gysegem, P.; Schow, S.; Swyke, C. *J. Chem. Soc., Dalton* **1975**, 16. An intermediate was also characterized via UV−vis spectra in (b), but the authors proposed a linear structure for the intermediate.
(22) Kovács, J.; Pintér, I.; Kajtár-Peredy, M.; Somsák, L. *Tetrahedron* **1997**, *44*, 15041.
(23) (a) Chung, M.-K.; Orlova, G.; Goddard, J. D.; Schlaf, M.; Harris, R.; Beveridge, T. J.; White, G.; Hallett, F. R. *J. Am. Chem. Soc.* **2002**, *124*, 10508 (b) Mayo, P.; Orlova, G.; Goddard, J. D.; Tam, W. *J. Org. Chem.* **2001**, *66*, 5182. (c) Hoon-Khosla, M.; Fawcett, W. R.; Goddard, J. D.; Tian, W.-Q.; Lipkowski, J. *Langmuir* **2000**, *16*, 2356. (d) Bettinger, H. F.; Sulzbach, H. M.; Schleyer, P. v. R.; Schaefer, H. F., III. *J. Org. Chem.* **1999**, *64*, 3278. (e) Woodcock, H. L.; Moran, D.; Schleyer, P. v. R.; Schaefer, H. F., III. *J. Am. Chem. Soc.* **2001**, *123*, 4331. (f) Gilbert, T. M.; Hristov, I.; Ziegler, T. *Organometallics* **2001**, *20*, 1183.
(24) (a) Cui, Q.; Karplus, M. *J. Am. Chem. Soc.* **2001**, *123*, 2284. (b) Smedarchina, Z.; Siebrand, W.; Fernández-Ramos, A.; Cui, Q. *J. Am. Chem. Soc.* **2003**, *125*, 243. (c) Li, G.; Cui, Q. *J. Am. Chem. Soc.* **2003**, *125*, 15028.
(25) (a) Adachi, M.; Nagao, Y. *Chem. Mater.* **2001**, *13*, 662. (b) Shimizu, A.; Takada, S.; Shimooka, H.; Takahashi, S.; Kohiki, S.; Arai, M.; Oku, M. *Chem. Mater.* **2002**, *14*, 3971. (c) Rocquefelte, V.; Boucher, F.; Gressier, P.; Ouvrard, G. *Chem. Mater.* **2003**, *15*, 1812. (d) Carlier, D.; Van der Ven, A.; Delmas, C.; Ceder, G. *Chem. Mater.* **2003**, *15*, 2651.
(26) Alajarin, M.; Conesa, C.; Rzepa, H. S. *J. Chem. Soc., Perkin Trans.* **1999**, *2*, 1811.
(27) Pople, J. A.; Head-Gordon, M.; Raghavachari, K. *J. Chem. Phys.* **1987**, *87*, 5968.
(28) (a) Ditchfield, R.; Hehre, W. J.; Pople, J. A. *J. Chem. Phys.* **1971**, *54*, 724. (b) Hehre, W. J.; Ditchfield, R.; Pople, J. A. *J. Chem. Phys.* **1972**, *56*, 2257. (c) Hariharan, P. C.; Pople, J. A. *Mol. Phys.* **1974**, *27*, 209. (d) Gordon, M. S. *Chem. Phys. Lett.* **1980**, *76*, 163. (e) Pople, J. A.; Head-Gordon, M.; Raghavachari, K. *Chem. Phys. Lett.* **1987**, *89*, 7382.
(29) Møller, C.; Plesset, M. S. *Phys. Rev.* **1934**, *46*, 618.
(30) Becke, A. D. *J. Chem. Phys.* **1993**, *98*, 5648.
(31) (a) Lee, C.; Yang, W.; Parr, R. G. *Phys. Rev. B* **1988**, *37*, 785. (b) Miehlich, B.; Savin, A.; Stoll, H.; Preuss, H. *Chem. Phys. Lett.* **1989**, *157*, 200.

initial attack, and the details for the relative stability of the *cis*- and *trans*-intermediates with different substituent groups. To study the substitution effects, we have replaced H atoms of PH_3 and N_3H with methyl (CH_3), ethyl (C_2H_5), *tert*-butyl ($C(CH_3)_3$), and phenyl (C_6H_5) groups and fluorine (F) atoms, respectively.

II. Computational Methods

The quantum chemical package Gaussian 98[33] was employed for the calculations. All stationary points were fully optimized at the B3LYP/6-31G(d) level. The B3LYP level of theory uses Becke's 3-parameter general gradient approximation (GGA) exchange functional[30] mixed with the exact (Hartree−Fock) exchange and the Lee−Yang−Parr GGA correlation functional.[31] The Hessian was calculated to verify the nature of the stationary points on potential energy surface, i.e., all positive eigenvalues for a minimum and one and only one negative eigenvalue for a transition state. Intrinsic reaction coordinate (IRC)[34] calculations were performed for a transition state if the two stationary points connecting this transition state were not clearly known. When IRC calculations could not produce the two connected stationary points, geometry optimization with the geometry of the first step IRC or with a distorted geometry of the transition state along its negative eigenvector was performed to reach a stationary point. The Gibbs free energy analysis was performed at 298 K and 1 atm pressure. Natural charge analysis using NBOs[35] was performed with B3LYP/6-31G(d). The performance of the B3LYP method with 6-31G(d) basis set was well studied to produce reliable theoretical results.[36]

III. Results and Discussion

There are two possibilities for the phosphorus atom to attack the external nitrogen N_α far from the substituent group on N_γ of N_3R.[14,20] The *trans* direction is from same side of the substituent group R on N_γ of N_3R, and the *cis* direction is from the backside of the substituent group R on N_γ of N_3R (Scheme 2). Here, questions naturally arise: which direction is the preferable reaction pathway for the Staudinger reaction and why? Previous ab initio studies on the Staudinger reaction of $PH_3 + N_3H$[26] revealed that the energy of the *trans*-transition state is 25 kcal/mol higher than that of the *cis*-transition state; hence the *cis*-reaction pathway is favored.

SCHEME 2

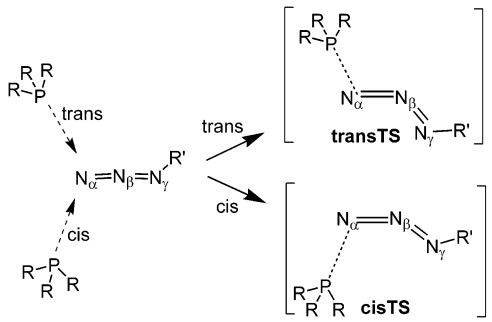

SCHEME 3

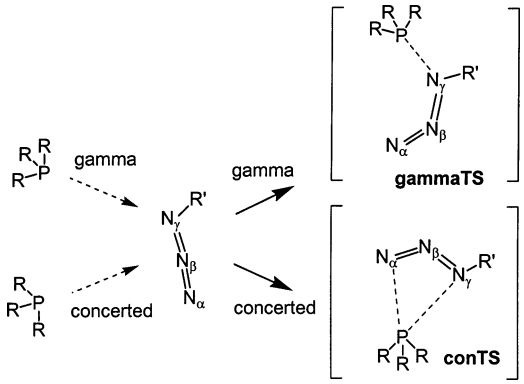

However, two additional questions remain to be resolved: (1) If the N_γ-attacking reaction mechanism exists? (2) Is it possible for P to attack N_α and N_γ at the same time? If so, what are the energy profiles for these two reaction pathways?

A. Initial Reaction. The reaction profile for the parent reaction ($PH_3 + N_3H$) is shown in Figure 1, and the relative energies with the ZPVE correction and Gibbs free energies of the stationary points on the reaction profiles to those of the reactants are listed in Tables 1 and 2. To account for the temperature effect, we have based our discussions on the Gibbs free energies thereafter.

At the B3LYP level of theory, the initial *trans*-reaction barrier is 26.4 kcal/mol higher than that of the initial *cis*-reaction barrier. Even the energy of the *trans*-intermediate (**trans**) that forms right after the initial *trans*-transition state (**transTS**) is 5.5 kcal/mol higher than the initial *cis*-transition state (**cisTS**). Our studies on the parent Staudinger reaction agree with the previous calculations on the preferred reaction pathway.[26] The energy difference between the initial *trans*- and *cis*-reaction barriers are so large that an essential impasse is left for the *trans*-reaction pathway in the Staudinger reaction of $PH_3 + N_3H$ at ordinary conditions.

(32) (a) Hohenberg, P.; Kohn, W. *Phys. Rev.* **1964**, *136*, B864. (b) Kohn, W.; Sham, L. J. *Phys. Rev.* **1965**, *40*, A1133. (c) Parr, R. G.; Yang, W. *Density-Functional Theory of Atoms and Molecules*; Oxford University Press: New York, 1989.

(33) Frisch, M. J.; Trucks, G. W.; Schlegel, H. B.; Scuseria, G. E.; Robb, M. A.; Cheeseman, J. R.; Zakrzewski, V. G.; Montgomery, J. A., Jr.; Stratmann, R. E.; Burant, J. C.; Dapprich, S.; Millam, J. M.; Daniels, A. D.; Kudin, K. N.; Strain, M. C.; Farkas, O.; Tomasi, J.; Barone, V.; Cossi, M.; Cammi, R.; Mennucci, B.; Pomelli, C.; Adamo, C.; Clifford, S.; Ochterski, J.; Petersson, G. A.; Ayala, P. Y.; Cui, Q.; Morokuma, K.; Malick, D. K.; Rabuck, A. D.; Raghavachari, K.; Foresman, J. B.; Cioslowski, J.; Ortiz, J. V.; Stefanov, B. B.; Liu, G.; Liashenko, A.; Piskorz, P.; Komaromi, I.; Gomperts, R.; Martin, R. L.; Fox, D. J.; Keith, T.; Al-Laham, M. A.; Peng, C. Y.; Nanayakkara, A.; Gonzalez, C.; Challacombe, M.; Gill, P. M. W.; Johnson, B. G.; Chen, W.; Wong, M. W.; Andres, J. L.; Head-Gordon, M.; Replogle, E. S.; Pople, J. A. *Gaussian 98*, revision A.9; Gaussian, Inc.: Pittsburgh, PA, 1998.

(34) (a) Fukui, K. *Acc. Chem. Res.* **1981**, *14*, 363. (b) Gonzalez, C.; Schlegel, H. B. *J. Chem. Phys.* **1989**, *90*, 2154. (c) Gonzalez, C.; Schlegel, H. B. *J. Phys. Chem.* **1990**, *94*, 5523.

(35) Reed, A. E.; Curtiss, L. A.; Weinhold, F. *Chem. Rev.* **1988**, *88*, 899.

(36) (a) Sheng, Y.; Musaev, D. G.; Reddy, K. S.; McDonald, F. E.; Morokuma, K. *J. Am. Chem. Soc.* **2002**, *124*, 4149. (b) Vereecken, L.; Peeters, J.; Bettinger, H. F.; Kaiser, R. I. Schleyer, P. v. R.; Schaefer, H. F., III. *J. Am. Chem. Soc.* **2002**, *124*, 2781. (b) Musaev, D. G.; Morokuma, K. *J. Phys. Chem.* **1996**, *100*, 6509. (c) Erikson, L. A.; Pettersson, L. G. M.; Siegbahn, P. E. M.; Wahlgren, U. *J. Chem. Phys.* **1995**, *102*, 872. (d) Li, J.; Schreckenbach, G.; Ziegler, T. *J. Am. Chem. Soc.* **1995**, *117*, 486. (e) Cui, Q.; Musaev, D. G.; Svensson, M.; Sieber, S.; Morokuma, K. *J. Am. Chem. Soc.* **1995**, *117*, 12366. (f) Heinemann, C.; Hertwig, R. H.; Wesendrup, R.; Koch, W.; Schwarz, H. *J. Am. Chem. Soc.* **1995**, *117*, 495. (g) Hertwig, R. H.; Hrusak, J.; Schroder, D.; Koch, W.; Schwarz, H. *Chem. Phys. Lett.* **1995**, *236*, 194. (h) Schroder, D.; Hrusak, J.; Hertwig, R. H.; Koch, W.; Schwerdtfeger, P.; Schwarz, H. *Organometallics* **1995**, *14*, 312. (i) Berces, A.; Ziegler, T.; Fan, L. *J. Phys. Chem.* **1994**, *98*, 1584. (j) Ricca, A.; Bauschlicher, C. W., Jr. *J. Phys. Chem.* **1994**, *98*, 12899. (k) Fiedler, A.; Schroder, D.; Shaik, S.; Schwarz, H. *J. Am. Chem. Soc.* **1994**, *116*, 10734.

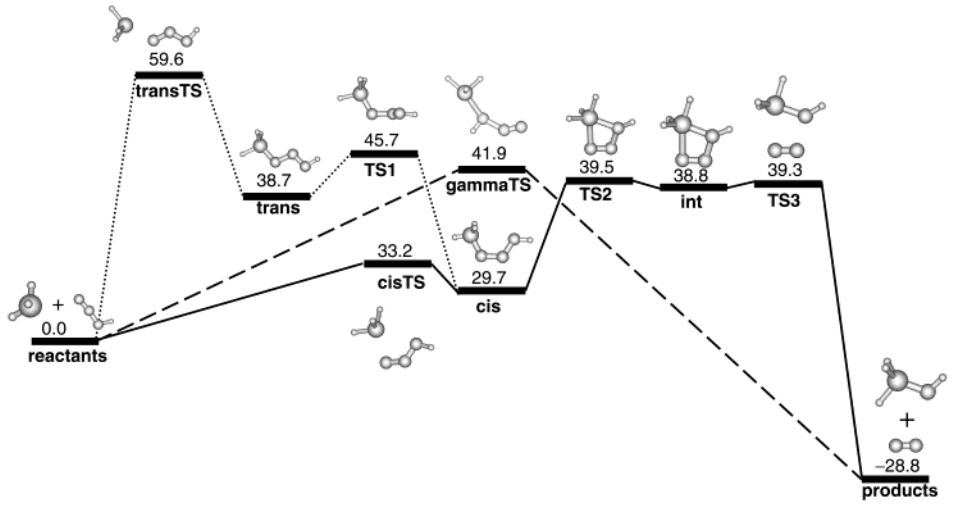

FIGURE 1. Schematic reaction profiles of the Staudinger reaction of $PH_3 + N_3H$. The numbers are relative Gibbs free energies (in kcal/mol) of stationary points (measured with respect to the total Gibbs free energy of the reactants).

TABLE 1. Relative Energies of Stationary Points to That of Reactants for the Staudinger Reactions, Predicted at the B3LYP/6-31G(d) Level of Theory[a]

R in PR_3	R in N_3R	gammaTS	transTS	cisTS	trans	TS1	cis	TS2	int	TS3	products
H	H	33.4(41.9) −779.5	50.3(59.6) −580.3	23.9(33.2) −324.2	29.3(38.7)	36.0(45.7) −199.6	19.9(29.7)	29.4(39.5) −233.2	29.0(38.8)	28.8(39.3) −479.2	−29.2(−28.8)
CH_3	H	26.5(36.4) −734.9	36.7(47.0) −419.1	13.4(23.7) −225.5	5.7(16.8)	13.5(24.9) −197.2	1.4(12.8)	17.9(30.2) −153.6	16.8(28.7)	17.4(29.2) −459.7	−49.5(−47.7)
C_2H_5	H	26.0(37.0) −728.8	37.0(48.9) −421.5	13.1(24.4) −214.2	5.1(17.4)	12.4(25.0) −191.6	1.3(13.9)	19.7(33.8) −101.4	17.6(31.3)	18.1(31.3) −436.1	−50.1(−47.2)
$C(CH_3)_3$	H	25.9(36.1) −703.1	35.0(44.8) −388.5	11.5(23.0) −197.5	3.0(14.9)	11.0(23.5) −206.4	3.1(15.5)	29.3(41.7) −150.3	27.7(39.7)	24.5(40.9) −387.7	−51.0(−48.7)
C_6H_5	H	26.5(37.3) −732.5	36.7(47.8) −396.8	13.3(24.9) −216.8	7.5(19.5)	15.5(27.7) −184.9	4.1(16.9)	21.3(34.8) −133.6	20.8(33.7)	21.6(34.7) −451.4	−47.8(−45.3)
CH_3	C_6H_5	32.3(43.0) −712.5	33.0(44.3) −344.8	10.7(21.5) −194.9	1.9(13.2)	10.4(22.5) −181.2	−2.4(9.8)	18.0(31.1) −33.5	**cis**[c]	18.2(30.9) −289.1	−50.6(−48.3)
CH_3	F	17.9(27.8) −642.8	12.5(23.5) −290.2	0.9(11.1) −99.3	−21.5(−9.7)	−14.1(−1.8) −175.5	−21.9(−9.7)	**TS3**[b]	**cis**	4.8(17.6) −173.4	−54.7(−52.7)
C_6H_5	C_6H_5	32.6(44.6) −718.2	32.7(44.9) −319.2	10.8(22.9) −184.9	3.6(16.7)	12.3(25.3) −166.7	0.6(14.5)	NF[d]	**cis**	24.4(39.5) −320.2	−48.6(−45.5)
F	F	21.1(31.1) −626.6	24.8(35.8) −357.1	12.5(22.9) −276.1	−6.6(4.5)	−2.5(9.2) −114.3	−6.2(5.3)	**TS3**	**cis**	10.4(22.8) −219.6	−44.1(−39.5)
CH_3	CH_3	31.3(42.0) −739.1	35.7(47.0) −393.7	13.1(23.7) −226.3	1.7(14.4)	9.6(21.9) −161.2	−1.4(11.0)	16.4(29.4) −110.2	15.5(27.8)	16.5(29.0) −350.2	−45.1(−42.9)

[a] All electronic energies (in kcal/mol) are outside of parenthesis and are corrected for the zero point vibrational energy (ZPVE). All Gibbs free energies (in kcal/mol) are in the bracket and are calculated at 298 K and 1 atm. The first row shows the relative energies and the second row shows the wave numbers of the imaginary vibrational frequencies (in cm^{-1}) for the transition states. [b] **TS3**: started from similar geometry of **TS2**, only **TS3** could be found. [c] **cis**: started from similar geometry of **int**, only **cis** could be found. [d] NF: not found. Only a second saddle point has been found. One of the two negative eigenvalues, 41.5(*i*) cm^{-1}, of Hessian is the PN bond stretching and the other negative eigenvalue, 31.4(*i*) cm^{-1}, is the rotation of benzene rings on P about the PC bonds.

The structures of **transTS** and **cisTS** can give a partial explanation on the greater stability of **cisTS**. In azide N_3R, the three nitrogen atoms are almost linear (the A_{NNN} angel is 171.6°); any further bending of the NNN backbone will destabilize this molecule. The A_{NNN} angle (as shown in Figure 1) in **cisTS** is 126.6° and in **transTS** is 125.8°. From this angle alone, one will conclude that **transTS** is more stable than **cisTS**. On the other hand, a closer look at the structures of these two transition states (as shown in Figures 1 and 2) reveals that there might be some extra interaction between the phosphorus atom in PH_3 and the hydrogen-bonded nitrogen N_γ in N_3H for **cisTS**, which does not exist for **transTS**. In **cisTS**, the PN_γ bond distance $R_{PN\gamma}$ is just 0.61 Å longer than the PN_α bond distance $R_{PN\alpha}$. The partial charges from the NBO natural partial charge analysis on P and N_γ have opposite signs, resulting an electrostatic attraction. The NBO natural partial charge analysis additionally indicates that there exists a transfer of about 0.46 electrons from the PH_3 subunit to the N_3H subunit in **cisTS**.

Molecular orbital analysis on **cisTS** (as shown in Figure 2) further manifests a strong bonding interaction between P and N_γ. The highest occupied molecular orbital (HOMO) of **cisTS** is an anti-bonding π orbital with a node on one of two central nitrogen atoms, N_β. The orbital right below the HOMO (HOMO-1) is mainly a σ-overlap between the p orbitals on both P and N_γ. The second orbital below the HOMO (HOMO-2) is another strong σ-overlap between P and N_α. The low-lying σ-overlaps in the HOMO-1 and the HOMO-2 certainly stabilize **cisTS**.

In **transTS**, the HOMO is the overlap of the in-plane (PNNN plane) p orbitals of PNNN and looks more like a π-overlap rather than a σ-overlap. The HOMO-1 is a π

TABLE 2. Reaction Barriers for cis to Overcome Transition States cisTS, TS1, and TS3 for the Staudinger Reactions, Predicted at the B3LYP/6-31G(d) Level of Theory[a]

PR_3	N_3R	ΔE (**cis→cisTS**)	ΔG (**cis→cisTS**)	ΔE (**cis→TS1**)	ΔG (**cis→TS1**)	ΔE (**cis→TS3**)	ΔG (**cis→TS3**)
H	H	4.0	3.5	16.1	16.0	8.9	9.6
CH_3	H	12.0	10.9	12.1	12.1	16.0	16.4
C_2H_5	H	11.8	10.5	11.1	11.1	16.8	17.4
$C(CH_3)_3$	H	8.4	7.5	7.9	8.0	21.4	25.4
C_6H_5	H	9.2	8.0	11.4	10.8	17.5	17.8
CH_3	C_6H_5	13.1	11.7	12.8	12.7	20.6	21.1
CH_3	F	22.8	20.8	7.8	7.9	26.7	27.3
C_6H_5	C_6H_5	10.2	8.4	11.7	10.8	23.8	25.0
F	F	18.7	17.4	3.7	3.9	16.6	17.5
CH_3	CH_3	14.5	12.7	11.0	10.9	17.9	18.0

[a] All energies (in kcal/mol) are corrected for the zero point vibrational energy (ZPVE), and Gibbs energies are calculated at 298 K and 1 atm.

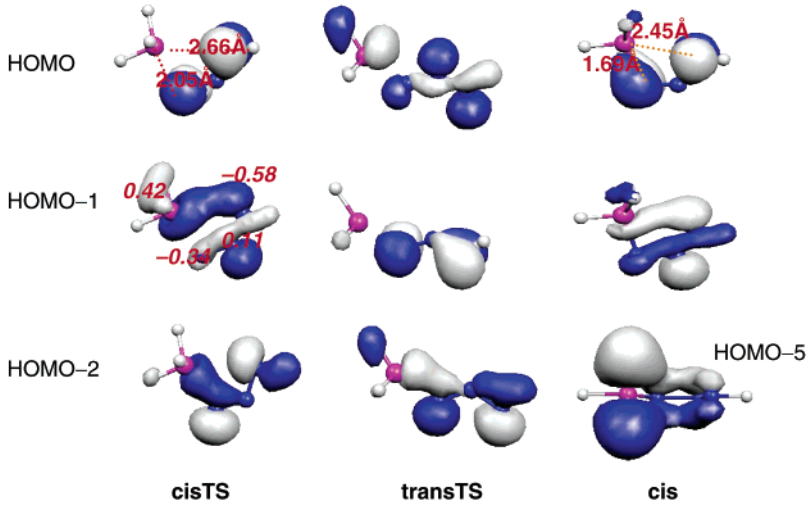

FIGURE 2. Relevant molecular orbitals of the *cis*-transition state (**cisTS**), the *trans*-transition state (**transTS**), and the *cis*-intermediate (**cis**) for the Staudinger reaction of $PH_3 + N_3H$. HOMO-*n* is the *n*th occupied orbital below the HOMO. The numbers on the HOMO are bond distances of P to N_α and N_γ, respectively. The numbers on the HOMO-1 are the NBO natural partial charges.

orbital of $N_\alpha N_\beta N_\gamma$, and the HOMO-2 is also a π-orbital-like overlap of the lone-pair electrons of $PN_\alpha N_\beta N_\gamma$ with a node at N_β.

Obviously, the bonding between P and N_γ in **cisTS** stabilizes **cisTS**, whereas in **transTS** there is no such stabilization. With molecular orbital analysis, the relative stability of the *trans*- and the *cis*-initial transition states and the preference of the initial reaction are clearly addressed.

The N_γ-attacking mechanism indeed exists. It is a one-step reaction mechanism. In this one-step transition state, **gammaTS** (as shown in Figure 1), the phosphane attacks N_γ, PN bond forms, $N_\beta N_\gamma$ bond breaks and N_2 molecule leaves simultaneously. There is no doubt that this reaction barrier is higher than the *cis* pathway (as shown in Table 1), since this transition state has one bond forming and one bond breaking. There does not exist additional stabilization effect in the one-step transition state.

Among the three initial reaction pathways, the *cis*-initial reaction has the lowest reaction barrier, the *trans*-initial reaction has the highest one, and the one-step reaction lies between. Thus, the Staudinger reaction will go through the *cis*-initial reaction pathway.

B. Last Stage. After overcoming the initial reaction barrier, the system reaches the *cis*-intermediate (**cis**). The PN_α bond distance $R_{PN\alpha}$ reduces from 2.05 Å in **cisTS** to 1.69 Å in **cis**, and the PN_γ bond distance $R_{PN\gamma}$ reduces from 2.66 Å in **cisTS** to 2.45 Å in **cis**. Electron transfer from the PH_3 subunit to the N_3H subunit increases as PH_3 moves closer to N_3H. In **cis**, P only bonds to N_α; the distance between P and N_γ is 2.45 Å, which is too long to be regarded as an ordinary chemical bond. The bonding of P to nitrogen atoms of N_3H in **cis** can shift from N_α to N_γ through a P-atom-shifting transition state (**TS2**), with a barrier of 9.8 kcal/mol with respect to **cis**, and the system reaches an intermediate (**int**). In **TS2**, P bonds to both N_α and N_γ with bond distances of 1.94 and 1.85 Å, respectively, and P and the three nitrogen atoms form a four-membered ring, with an A_{NNN} angle of 107.1°. The structure of **int** is very similar to that of **TS2**. The two PN bond distances $R_{PN\alpha}$ and $R_{PN\gamma}$ in **int** are 1.96 and 1.75 Å, respectively, and the A_{NNN} angle is 104.5°. Because of the similarity in the structures of **TS2** and **int**, their energies are very close to each other: **int** is only 0.4 kcal/mol slightly more stable than **TS2**.

As noticed in a previous study,[20] the $PN_\alpha N_\beta N_\gamma$ four-membered ring is not planar in **TS2** ($D_{PNNN} = -10.7°$) and **int** ($D_{PNNN} = 5.5°$). The last step of the Staudinger reaction is the dissociation of N_2 from the reaction complex through a N_2-dissociation transition state, **TS3**. The nature of **TS3** can be seen from the two bond

TABLE 3. Natural Charges of Phosphorus Atom in the Phosphane Unit and Nitrogen Atoms in the Azide Unit of cisTS Transition State for the Staudinger Reactions, Predicted at the B3LYP/6-31G(d) Level of Theory[a]

R in PR_3	R in N_3R	P	N_α	N_β	N_γ	CT	$P-N_\alpha$
H	H	+0.42 (+0.01)	−0.34 (−0.05)	+0.11 (+0.20)	−0.58 (−0.54)	0.46	2.052
CH_3	H	+1.15 (+0.85)	−0.26 (−0.05)	+0.11 (+0.20)	−0.59 (−0.54)	0.38	2.258
C_2H_5	H	+1.13 (+0.84)	−0.25 (−0.05)	+0.11 (+0.20)	−0.60 (−0.54)	0.37	2.302
$C(CH_3)_3$	H	+1.15 (+0.81)	−0.29 (−0.05)	+0.10 (+0.20)	−0.61 (−0.54)	0.45	2.266
C_6H_5	H	+1.23 (+0.90)	−0.29 (−0.05)	+0.11 (+0.20)	−0.59 (−0.54)	0.41	2.225
CH_3	C_6H_5	+1.12 (+0.85)	−0.20 (−0.04)	+0.12 (+0.22)	−0.36 (−0.31)	0.36	2.315
CH_3	F	+1.04 (+0.85)	−0.14 (+0.04)	+0.10 (+0.15)	−0.03 (+0.04)	0.28	2.437
C_6H_5	C_6H_5	+1.20 (+0.90)	−0.23 (−0.04)	+0.12 (+0.22)	−0.37 (−0.31)	0.39	2.275
F	F	+2.01 (+1.71)	−0.29 (+0.04)	+0.10 (+0.15)	+0.06 (+0.04)	0.37	2.105
CH_3	CH_3	+1.14 (+0.85)	−0.26 (−0.07)	+0.11 (+0.21)	−0.39 (−0.33)	0.37	2.257

[a] CT is charges transferred from PR_3 to N_3R. $P-N_\alpha$ is the distance (in Å) between P and N_α in **cisTS**. The numbers in parenthesis are the natural charges of P and N atoms in isolated phosphanes and azides

distances: $R_{PN\alpha} = 2.06$ Å and $R_{N\beta N\gamma} = 1.60$ Å, which are similar to previous predictions with the same method.[26] The energies of **TS3** and **int** are so close that the system does not even need to overcome any reaction barrier to dissociate the N_2 molecule. With the ZPVE correction, the (electronic) energy of **TS3** is 0.2 kcal/mol *lower* than that of **int**. Without the ZPVE correction, the (electronic) energy of **TS3** is 1.5 kcal/mol *higher* than that of **int**. Calculations with a larger basis set[26] and with higher level of theory[20] had similar predictions on the relative stability of these two stationary points. Hence, we conclude that the potential energy surface for this particular region is so flat that the system dissociates N_2 immediately after overcoming the reaction barrier of **TS2**. So, the overall reaction profile for the Staudinger reaction essentially goes through two stages: (i) **cisTS**, and (ii) **TS2** together with **TS3**, with one intermediate, **cis**, between them. This understanding for the Staudinger reaction confirms the conventional reaction mechanism proposed almost 4 decades ago.[14]

Quite curiously, the dihedral angle D_{PNNN} is 2.5° in **TS3**, deviating from the previous prediction.[20] It turns out that the transition state located in the previous study[20] is not for N_2 dissociation. We reproduced the planar structure of **TS3** of ref 20 with MP2(full)/6-31G-(d) and found that the previously identified transition state[20] is simply an out-of-plane (PNNN plane) bending of the HN_γ bond. One can easily notice that both $R_{PN\alpha}$ (1.95 Å) and $R_{N\beta N\gamma}$ (1.43 Å) bond distances in ref 20 are shorter than those predicted in the present work. In the actual last transition state, the D_{PNNN} dihedral angle is 3.7°, and the $R_{PN\alpha}$ and $R_{N\beta N\gamma}$ bond distances are 2.03 and 1.59 Å, respectively, at MP2(full)/6-31G(d) level of theory.

C. trans and cis. As depicted in Figure 1, if the Staudinger reaction follows the initial *trans*-transition state (**transTS**), it will reach a *trans*-intermediate (**trans**). The overall structure of **trans** is similar to that of **transTS**. Going through a transition state (**TS1**) with an internal rotation about the $N_\alpha N_\beta$ bond, **trans** can isomerize to **cis** with a barrier of 7.0 kcal/mol. In other words, **cis** can isomerize to **trans** with a higher reaction barrier of 16.0 kcal/mol, since **cis** is 9.0 kcal/mol more stable than **trans**. The factors determining the relative stability of **trans** and **cis** are similar to those between **cisTS** and **transTS**. A slight difference is that the bonding of P to the N_3H subunit stabilizes both **trans** and **cis** intermediates; the extra stabilization for **cis** mainly comes from the σ-overlap between P and N_γ, as illustrated in Figure 2. The frontier molecular orbitals of **trans** are very similar to those of **transTS**, except for the HOMO-1 of **trans**, which is a π orbital with a node between N_α and N_β. This π orbital runs over from P to N_α and from N_β to N_γ. One should also note that the compact conformation of **cis** to some degree introduces additional ring tension for $PN_\alpha N_\beta N_\gamma$ and destabilizes **cis**. Another factor of stabilization effect is the electrostatic interaction between P and N_γ in **cis**, which depends on the nature of substituents on P and N_γ. For $PH_3 + N_3H$, the electrostatic interaction in **cis** between P and N_γ is attractive, because of the opposite signs of the partial charges on P and N_γ. The overall stability of **cis** is a compromise between the factors of stabilization and destabilization.

D. Substitution Effects. According to the electronegativities of elements (H 2.30, C 2.54, N 3.07, F 4.19, P 2.25),[37] all of the substituents studied in the present work are electron-withdrawing groups with respect to P and are electron-donating groups with respect to N, except for the strong electron-withdrawing F. The substituents on PR_3 are fluorine (F),[38] methyl (CH_3), ethyl (C_2H_5), *tert*-butyl ($C(CH_3)_3$), and phenyl (C_6H_5) groups. The substituents on N_3R are fluorine (F),[39] methyl (CH_3), and phenyl (C_6H_5) groups. We have investigated 11 Staudinger reactions with different substituents on PR_3 and N_3R.

As displayed in Tables 1 and 2, the initial reaction barriers of the substituted Staudinger reactions drop at least 10 kcal/mol (except for the reactions with F substituent) for both the *trans*- and the *cis*-reaction pathways, and the reaction barrier for the *trans*-reaction pathway is at least 10 kcal/mol higher than that of the

(37) Allen, L. C. *Int. J. Quantum Chem.* **1994**, *49*, 253.

(38) Experimental studies on PF_3: (a) Jürgensen, A.; Cavell, R. G. *J. Electron Spectrosc. Relat. Phenom.* **2003**, *128*, 245. (b) Woska, D.; Prock, A.; Giering, W. P. *Organometallics* **2000**, *19*, 4629. (c) Jones, R. G.; Abrams, N. E.; Jackson, G. J.; Booth, N. A.; Butterfield, M. T.; Cowie, B. C. C.; Woodruff, D. P.; Crapper, M. D. *Surf. Sci.* **1998**, *414*, 396. Theoretical studies: (a) Moc, J. *Chem. Phys. Lett.* **2002**, *363*, 328. (b) Lau, J. K.-C.; Li, W.-K. *THEOCHEM* **2002**, *578*, 221.

(39) Experimental studies on N_3F: (a) Schatte, G.; Willner, H.; Willert-Porada, M. *Magn. Reson. Chem.* **1992**, *30*, 118. (b) Schatte, G.; Willner, H. *Z. Naturforsch., B: Chem. Sci.* **1991**, *46*, 483. (c) Christen, D.; Mack, H. G.; Schatte, G.; Willner, H. *J. Am. Chem. Soc.* **1988**, *110*, 707. Experimental studies on other azides (N_3H, N_3Cl, N_3CF_3, N_3Cl, and N_3CN): (d) Harmony, M. D.; Laurie, V. M.; Kuczowski, R. L.; Swendeman, R. H.; Ramsay, D. A.; Lovas, F. J.; Lafferty, W. J.; Maki, A. G. *J. Phys. Chem. Ref. Data Ser.* **1979**, *8*, 619. (e) Christe, K. D.; Christen, D.; Oberhammer, Schack, C. J. *Inorg. Chem.* **1984**, *23*, 4283. (f) Winnewisser, B. P. *J. Mol. Spectrosc.* **1980**, *82*, 220. Theoretical studies: (i) Wang, L. J.; Warburton, P.; Mezey, P. G. *J. Phys. Chem. A* **2002**, *106*, 2748. (j) Chaban, G.; Yarkony, D. R.; Gordon, M. S. *J. Chem. Phys.* **1995**, *102*, 7983. (k) Otto, M.; Lotz, S. D.; Frenking, G. *Inorg. Chem.* **1992**, *31*, 3647.

cis-reaction pathway. The dropping of the initial reaction barrier upon substitutions on PR_3 and N_3R could be explained by the charge population change of phosphorus and nitrogen atoms from unsubstituted to substituted Staudinger reactions as shown in Table 3. In all of the Staudinger reactions of substituted phosphane, the phosphorus atom has much larger positive charges than that in PH_3, thus resulting in stronger electrostatic attractions, which stabilize **cisTS** and lower the initial reaction barrier. As a result of the steric effect and the fact that the phosphorus atom interacts only with N_γ in **gammaTS**, the one-step initial reaction barrier does not drop much in the substituted Staudinger reactions. The lowering of the initial reaction barrier could also be seen from the PN_α bond distance in **cisTS** as shown in Table 3. All of the substituted **cisTS** have a PN_α bond distance longer than that in the parent reaction. **cisTS** of the substituted Staudinger reactions is an earlier transition state and with less geometry distortion, which stabilizes **cisTS**. If we compare the PN_α bond distances and the *cis* reaction barriers, we could find some proportionality between the PN_α bond distances and reaction barriers.

For the reactions of $PR_3 + NH_3$ with substituents only on P, the different substituents [i.e., $P(CH_3)_3$, $P(C_2H_5)_3$, $P(C(CH_3)_3)_3$, and $P(C_6H_5)_3$] stabilize the stationary points similarly. From $P(CH_3)_3$ and $P(C_2H_5)_3$ to $P(C(CH_3)_3)_3$, the initial *cis*-reaction barriers have almost the same value. As the size of substituents on phosphanes gets bigger, the reaction barrier for the isomerization from **cis** to **trans** decreases, while the reaction barriers for N_2 dissociation increase substantially. The increase of the last-step reaction barrier is certainly due to the steric effect caused by the tension of the compact geometry of four-membered rings of the last three stationary points, **TS2**, **int**, and **TS3**.

Compared with the three alkyl groups, the phenyl-substituted Staudinger reaction, $P(C_6H_5)_3 + N_3H$, has an initial reaction barrier similar to the initial reaction barriers of the three alkyl-substituted Staudinger reactions and reaction barriers of the remaining steps similar to those of $P(C_2H_5)_3 + N_3H$ (see Tables 1 and 2). These four substituted Staudinger reactions are much more exothermic than the parent Staudinger reaction, $PH_3 + N_3H$, because the substituents provide some additional stabilization effect to the product ($R_3P{=}NH$).

The steric effect can also been found in the comparison of the reaction barriers of the last step between the Staudinger reactions of $P(C_6H_5)_3 + N_3C_6H_5$ and $P(CH_3)_3 + N_3CH_3$, the relative Gibbs free energies of **TS3** to **cis** in $P(C_6H_5)_3 + N_3C_6H_5$ is 7.0 kcal/mol higher than the relative Gibbs free energies of **TS3** to **cis** in $P(CH_3)_3 + N_3CH_3$. Such a relative Gibbs free energies in the Staudinger reaction of $P(CH_3)_3 + N_3C_6H_5$ lies between these two barriers. Overall, all alkyl-substituted Staudinger reactions have similar reaction profiles.

Because the potential energy surface around the last step of N_2 dissociation is very flat, some of the stationary points (**TS2** or **int**) have not been located at the B3LYP/6-31G(d) level of theory, e.g., for the Staudinger reactions of $P(CH_3)_3 + N_3C_6H_5$, $P(CH_3)_3 + N_3F$, $P(C_6H_5)_3 + N_3C_6H_5$, and $PF_3 + N_3F$. The energies of these three stationary points (**TS2**, **int**, and **TS3**) are very close to one another; the largest energy difference among these three conformations for the Staudinger reactions studied here is only 2.5 kcal/mol between **TS2** and **TS3** for $P(C_2H_5)_3 + N_3H$. According to this observation, the Staudinger reactions of these systems essentially take one step to dissociate N_2 after the formation of the **cis** intermediate.

The stabilization of substituents on the Staudinger reactions can be obviously seen from the substitution of F on the azide in the reaction of $P(CH_3)_3 + N_3F$. Both the *trans*- and the *cis*-initial reaction barriers drop more than 10 kcal/mol relative to their counterparts of the other systems investigated. All of the other stationary points for $P(CH_3)_3 + N_3F$ are also stabilized, as a result of the F substituent. This Staudinger reaction is the most exothermic. It also has the largest reaction barriers for its **cis** to reach the final products and to return to the initial reactants. The **cis** and **trans** intermediates in this reaction have the same relative stability (both are 9.7 kcal/mol lower than the reactants), and the isomerization barrier between these two **cis** and **trans** intermediates is also low (7.9 kcal/mol). This theoretical prediction agrees with the experimental result that both intermediates can be observed.[17−19] The other two F-substituted Staudinger reactions, $PF_3 + N_3F$ and $PF_3 + N_3CH_3$, are also stabilized by the substitution of F on the reactants.

The relative stability of **cis** to **trans** in all F-substituted Staudinger reactions drops significantly. In some reactions (e.g., $PF_3 + N_3F$), **trans** even becomes more stable than **cis**: F substituents stabilize **trans** more than **cis**. For the Staudinger reaction involving F-substituted azide (N_3F), positive partial charges on P and N_γ further destabilize **cis** through electrostatic repulsion between like charges. Some orbital overlap between P and N_β in **trans** stabilizes **trans** to a certain degree. The PN_α bond distance in **trans** is shorter than the same bond distance in **cis**. These factors reverse the relative stability of **trans** and **cis** in the Staudinger reaction of $N_3F + PF_3$.

As a result of the availability of the empty 3d orbital in P and lone-pair electrons on N, there are "special" π bonds in both **trans** and **cis**. The normal π on the $N_\alpha N_\beta N_\gamma$ unit extends to P to form a π orbital with a node between N_α and N_β, and this orbital is either the HOMO or the HOMO-1 (the first occupied orbital below the HOMO) in these systems (for example, see the HOMO of **cis** in $PH_3 + N_3H$ in Figure 2). Another π orbital is the combination of the π orbital of $N_\alpha N_\beta N_\gamma$ with two PC or PH σ orbitals, and this π orbital runs over the entire backbone of **trans** or **cis** (see the HOMO-5 of **cis** in $PH_3 + N_3H$ in Figure 2). The π orbital of $N_\alpha N_\beta N_\gamma$ can also extend to F in **trans** or **cis** of $N_3F + PF_3$. All the above π orbitals are normal π orbitals, because they distribute at the two sides of the PNNN plane. The "special" π orbital involves the lone-pair electrons of $N_\alpha N_\beta N_\gamma$ (p_x and p_y orbitals), PH (or PC or PF) and NH (or NF) σ orbitals (see the HOMO-1 of **cis** in $PH_3 + N_3H$ in Figure 2). Although this "special" π orbital distributes at the two sides of the PNNN backbone, it is in the PNNN plane. This "special" π orbital contributes to the σ overlaps between P and N_γ in **cis** and between P and N_β in **trans**. These "special" π bonds stabilize the intermediates so that these intermediates become observable in experiment.

Among the reaction barriers of **cis** to isomerize to **trans**, to reach the final products and to return to the reactants in the reaction of $P(C_6H_5)_3 + N_3C_6H_5$, the barrier of returning to the reactants is the smallest and the barrier of isomerizing to **trans** is the second smallest,

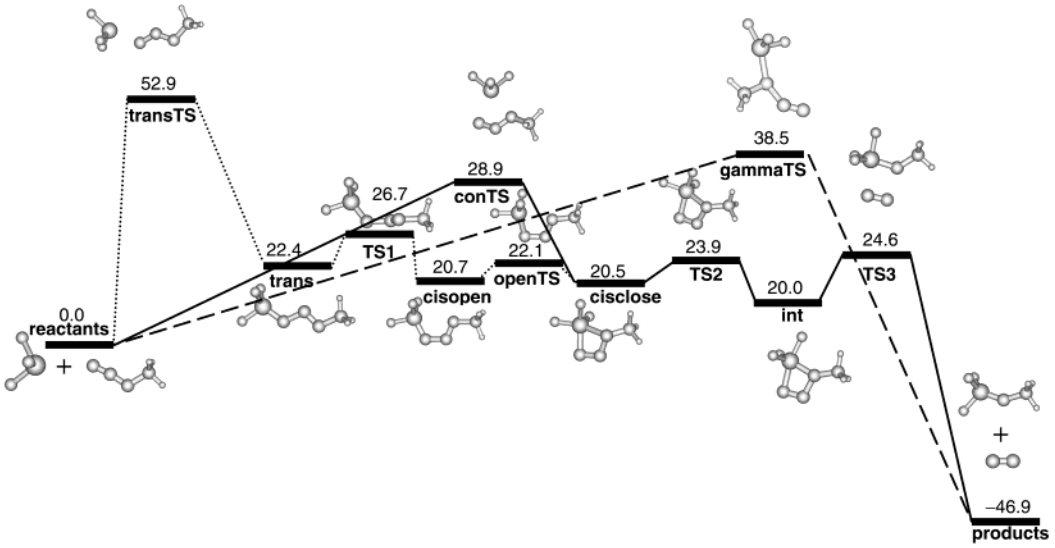

FIGURE 3. Schematic reaction profiles of the Staudinger reaction of $PF_3 + N_3CH_3$. The numbers are the relative Gibbs free energies (in kcal/mol) of stationary points to that of reactants (measured with respect to the total Gibbs free energy of the reactants).

TABLE 4. Relative Energies of Stationary Points to That of Reactants for the Staudinger Reaction of $PF_3 + N_3CH_3$, Predicted at the B3LYP/6-31G(d) Level of Theory[a]

	gammaTS	transTS	trans	TS1	cisopen	openTS	conTS	cisclose	TS2	int	TS3	products
electronic energy	27.4	41.8	11.3	14.8	9.1	9.7	18.3	9.2	11.1	8.0	12.7	−48.3
Gibbs energy	38.5	52.9	22.4	26.7	20.7	22.1	28.9	20.5	23.9	20.0	24.6	−46.9
imaginary frequency	−744.7	−436.6		−101.0		−83.6	−233.5		−80.7		−297.1	

[a] All electronic energies (in kcal/mol) are corrected for the zero point vibrational energy (ZPVE) and all Gibbs energies are calculated at 298 K and 1 atm. The last row shows the wave numbers (in cm^{-1}) of the imaginary vibrational frequencies for the transition states.

so the chance for observing the **cis** intermediate is larger than for **trans**, just like what has been observed in experiment.[14,18] The observation of a *trans*-intermediate was due to different substituents on P and N_γ,[16,17] or due to an extra coordination of transition metal (Mo or W) to N_α and N_γ,[15] which provides extra stabilization for **trans**.

E. New Reaction Profile for $PF_3 + N_3CH_3$. In **cisTS** of the Staudinger reaction of $PH_3 + N_3H$, $R_{PN\alpha}$ and $R_{PN\gamma}$ bond distances are 2.05 and 2.66 Å, respectively, and the overlap between P and N_γ is strong. With appropriate substituents on P and N_γ, P can attack N_α and N_γ simultaneously in **cisTS**. This is indeed the case for the Staudinger reaction of $PF_3 + N_3CH_3$. Instead of only attacking N_α in N_3CH_3, P attacks N_α and N_γ concurrently in the new initial transition state, **conTS**. The new reaction profile for the Staudinger reaction of $PF_3 + N_3CH_3$ is illustrated in Figure 3 and the relative energies are list in Table 4.

Still, the energy of **transTS** is much higher than that of **conTS**. **gammaTS** lies between **conTS** and **transTS**. In **conTS**, $R_{PN\gamma}$ (2.24 Å) is even shorter than $R_{PN\alpha}$ (2.29 Å), which means that P has a stronger bonding to N_γ than to N_α. This result agrees with the molecular orbital analysis on **conTS** (as shown in Figure 4): the overlap between P and N_γ is stronger than that between P and N_α. After overcoming **conTS**, the system reaches a more closed PNNN four-membered ring intermediate (**cisclose**) rather than the ordinary *cis*-intermediate (**cis**). **cisclose** can isomerize to an open *cis*-intermediate similar to **cis**, **cisopen**, through a transition state (**openTS**) for the

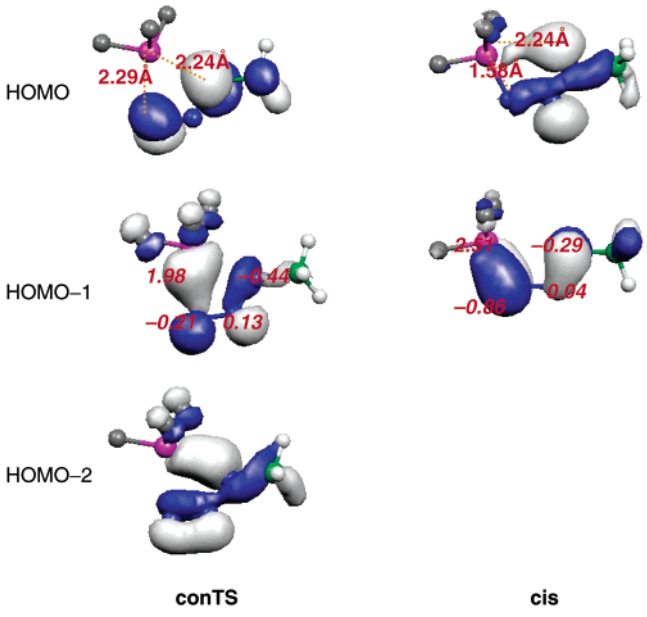

FIGURE 4. Frontier molecular orbitals of the concerted transition state (**conTS**) and the *cis*-intermediate (**cis**) for the Staudinger reaction of $PF_3 + N_3CH_3$. HOMO-*n* is the *n*th occupied orbital below the HOMO. The numbers on the HOMO are bond distances of P to N_α and N_γ, respectively. The numbers on the HOMO-1 are the NBO natural partial charges.

PNNN four-membered ring opening. Similar to the other Staudinger reactions, **cisopen** can isomerize to **trans** via

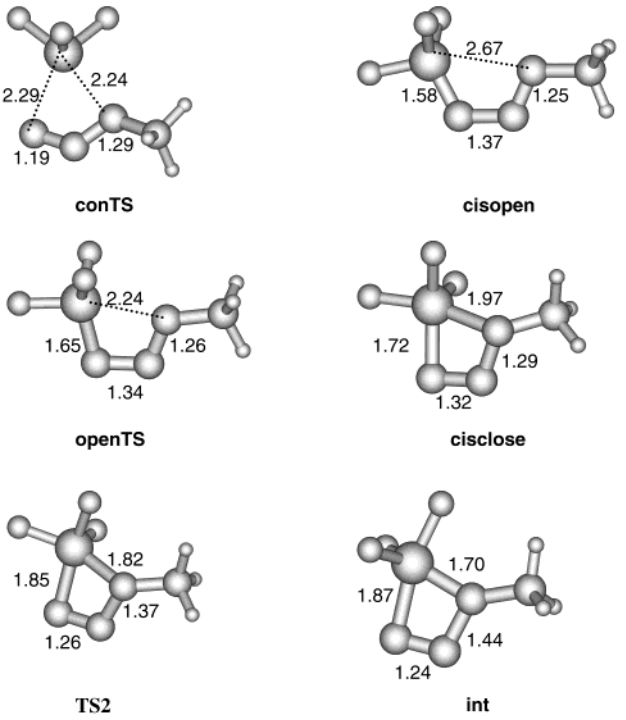

FIGURE 5. Structures of some stationary points in the Staudinger reaction of $PF_3 + N_3CH_3$, with bond distances (in Å). The assignment of the atoms is similar to the other figures.

a $N_\alpha N_\beta$ bond rotation. The structure of **cisclose** intimately resembles that of **int**: the $R_{PN\alpha}$ bond length in **cisclose** is 0.15 Å shorter than its counterpart in **int**, whereas $R_{PN\gamma}$ bond length is 0.27 Å longer in **cisclose** than that in **int**. Through a P-atom-shifting transition state (**TS2**), **cisclose** isomerizes to **int** with a 3.4 kcal/mol reaction barrier. It is worthy noticing that there are big π orbitals in **cisopen** and **trans**, which run over $N_\alpha N_\beta N_\gamma$ and the CH_3 group on N_γ and are similar to the big π orbital involving P and its substituents mentioned above in the other systems.

The process of the Staudinger reaction of $PF_3 + N_3CH_3$ can also be visualized from the bond distance changes along the reaction pathway. The major bond distances of these conformers are shown in Figure 5. From **cisopen** to **int**, PN_γ and $N_\alpha N_\beta$ bonds get shorter and PN_α and $N_\beta N_\gamma$ bonds get longer. After going over another transition state (**TS3**), **int** dissociates to $F_3P{=}NCH_3$ and N_2.

The overall reaction releases 46.9 kcal/mol Gibbs free energy. In this reaction, once the system overcomes the initial concerted reaction barrier (the largest reaction barrier), it will go through **TS2** and **TS3** and reach the final step rather than isomerizing to **trans**. The reaction barrier for **cisopen** to **trans** is higher than any reaction barrier for **cisclose** to reach the final products, $F_3P{=}NCH_3$ and N_2.

F. Solvent Effects and Basis Set Superposition Error. Solvent effects change conformational equililbria, reaction barriers, and molecular properties of chemical systems.[40] Since polar solvents were found to accelerate the Staudinger reactions,[14] the potential energy profile of a Staudinger reaction will change when solvent effects are taken into account.

We considered three Staudinger reactions for solvent effects: $PH_3 + N_3H$, $PF_3 + N_3CH_3$, and $P(CH_3)_3 + N_3F$. The latter two reactions can be considered as two extreme cases: very strong electron-withdrawing groups on phosphane and electron-donating group on azide, and the vice visa. We applied the Onsager dipole interaction model[41] on those reactions in dimethyl sulfoxide (DMSO), which was found to have a strong solvent effect on the Staudinger reactions.[12]

Geometry optimizations and frequency calculations were performed for the stationary points of the three Staudinger reactions in DMSO. The relative energies of the reactants and dipole moments of the stationary points are listed in Table 5. Because systems with large dipole moments have strong interactions with a polar solvent,[40] a polar solvent will provide more stabilization for more polar systems. Relative to the reactants (phosphane and azide), the energies of the intermediates and the transition states in the reaction of $PH_3 + N_3H$ lower slightly in DMSO. In another words, DMSO solvent stabilizes the intermediates and the transition states more with respect to the reactants in this reaction, thus decreasing the reaction barriers. The solvent stabilization varies with the magnitude of the dipole moments of the stationary points.[40,41] The initial *trans*-transition state and the *trans*-intermediate are stabilized more than the other stationary points as a result of their larger dipole moments. From Table 5, one can see that the dipole moments get larger in DMSO than in gas phase and that **trans** and **transTS** have the largest dipole moments.

In the Staudinger reaction of $PF_3 + N_3CH_3$, because of the strong electron-withdrawing nature of fluorine atoms, the dipole moments of all of the stationary points are smaller than those in the parent reaction, $PH_3 + N_3H$. Except for the P-atom-shifting transition state (**TS2**), all other stationary points in the Staudinger reaction of $PF_3 + N_3CH_3$ are destabilized in DMSO relative to the reaction in gas phase.

On the other hand, the Staudinger reaction of $P(CH_3)_3 + N_3F$ is much more stabilized in DMSO. This is reflected in the relative energies and dipole moment changes of the stationary points from gas phase to DMSO. More interestingly, the initial *trans*-transition state cannot be located in DMSO for the Staudinger reaction of $P(CH_3)_3 + N_3F$.[42] If we compare the relative energies and dipole moments of the stationary points in these three Staudinger reactions with one another, we find that adding electron-withdrawing groups to the azide and electron-donating

(40) (a) Wong, M. W.; Frisch, M. J.; Wiberg, K. B. *J. Am. Chem. Soc.* **1991**, *113*, 4776. (b) Wong, M. W.; Wiberg, K. B.; Frisch, M. J. *J. Am. Chem. Soc.* **1992**, *114*, 523. (c) Wong, M. W.; Wiberg, K. B.; Frisch, M. J. *J. Am. Chem. Soc.* **1992**, *114*, 1645.

(41) Onsager, L. *J. Am. Chem. Soc.* **1936**, *58*, 1486.

(42) We first used the optimized *trans*-transition state in gas phase as the initial geometry in DMSO, but the structure turns out to be a transition state for the dissociation of the F atom. Optimization with the elongated PN_α bond distance resulted in a transition state with a *cis*-conformation, which is the swinging movement of the azide subunit. The PN_α bond distance $R_{PN\alpha}$ is 3.02 Å in this transition state. The optimization of a structure distorted from the transition state along the negative eigenvector produces a *cis*-complex (a pre-reaction complex); this complex is also located in the gas phase with a similar structure in DMSO. We further constrained the PN_α bond distance to that of the *trans*-transition state in the gas phase (2.11 Å) and did constrained geometry optimization. In this constrained geometry optimization, the *trans*-structure turned to a *cis*-conformation in the end.

TABLE 5. Relative Energies to That of Reactants and Dipole Moments of Stationary Points for Staudinger Reactions of $PH_3 + N_3H$, $PF_3 + N_3CH_3$, and $P(CH_3)_3 + N_3F$, Predicted at the B3LYP/6-31G(d) Level of Theory in DMSO[a]

	gammaTS	transTS	trans	TS1	cisopen/cis[b]	openTS	conTS/cisTS[c]	cisclose	TS2	int	TS3	products
					$PH_3 + N_3H$							
gas phase	41.9	59.6	38.7	45.7	29.7		33.2		39.5	38.8	39.3	−28.8
	1.77	3.94	4.86	3.51	3.69		2.36		3.55	3.62	3.57	
DMSO	41.4	56.9	34.9	45.1	28.7		33.5		38.9	37.7	38.5	−31.2
	2.80	6.00	6.81	4.26	4.41		2.69		4.14	4.42	4.48	
					$PF_3 + N_3CH_3$							
gas phase	38.5	52.9	22.4	26.7	20.7	22.1	28.9	20.5	23.9	20.0	24.6	−46.9
	3.39	2.42	1.48	1.51	2.46	3.07	2.91	3.73	3.14	3.16	2.08	
DMSO	36.9	53.5	23.4	27.8	21.6	22.6	29.3	20.8	23.7	20.3	25.3	−45.8
	4.15	3.09	1.70	1.86	2.62	3.25	3.75	4.60	3.97	3.74	2.49	
					$P(CH_3)_3 + N_3F$							
gas phase	27.8	23.5	−9.7	−1.8	−9.7		11.1				17.6	−52.7
	3.64	7.72	8.19	6.94	7.18		5.26				5.07	
DMSO	25.7	NF	−16.6	−7.3	−15.5		7.9				15.2	−56.1
	5.40		10.6	8.95	9.28		6.14				6.14	

[a] The relative energies and dipole moments predicted in the gas phase are also listed for comparison. All Gibbs energies are calculated at 298 K and 1 atm. The first row shows the Gibbs energies, and the second row shows the dipole moments. Dipole moments are only listed for intermediates and transition states. [b] **cisopen**/**cis**: **cisopen** is for $P(CH_3)_3 + N_3F$, **cis** for $PF_3 + N_3CH_3$ and $PH_3 + N_3H$. [c] **conTS**/**cisTS**: **conTS** is for $P(CH_3)_3 + N_3F$, **cisTS** for $PF_3 + N_3CH_3$ and $PH_3 + N_3H$.

groups to the phosphane can accelerate the Staudinger reaction in polar solvents.

Finally, we studied the basis set superposition error (BSSE) for the Staudinger reactions and found this effect is quite small. We performed the BSSE correction for the initial *trans*-intermediate (**trans**) and the N_2-dissociation transition state (**TS3**) for the Staudinger reaction of $PH_3 + N_3H$. **trans** is an (PNNN) open structure, and **TS3** is a compact structure very different from the reactants. The two stationary points represent two typical extreme structures in the Staudinger reactions. The BSSE for these two stationary points are 2.8 and 3.1 kcal/mol, respectively. These two values indicate a more or less constant BSSE correction for all of the stationary points.

IV. Conclusions

In summary, the Staudinger reactions have been investigated within DFT. Overall, the Staudinger reaction goes through two major steps: (i) the system goes through an initial *cis*-transition state and reaches an intermediate, and (ii) the intermediate goes through a four-membered ring closure and N_2 dissociates. As a result of the flat potential energy surface in the second step, the Staudinger reaction essentially takes one step to dissociate N_2. Specifically, we have obtained the following new insights:

(1) The reason that the Staudinger reaction prefers the *cis*-reaction pathway has been thoroughly studied. The extra interaction between P with N_γ is the driving force for such a preference. Choosing appropriate substituents (electron-donating substituents) on the phosphane or (electron-withdrawing substituents) on the azide can facilitate the Staudinger reaction by lowering the initial reaction barrier.

(2) The relative stability of the *cis*- and the *trans*-intermediates has been explored. The overlap between P of PR_3 and N_γ of N_3R is the main factor for the stabilization of the *cis*-intermediate. The "special" π bond consisting of lone-pair electrons of $N_\alpha N_\beta N_\gamma$ and the big π bonds covering P contribute to the stability of the *cis*-intermediate. The change of substituents on the phosphane or the azide can change the relative stability of these two intermediates: **cis** and **trans**, since the substituents may stabilize **trans** more than they do for **cis**.

(3) An N_γ-attacking one-step reaction profile has been located for all the Staudinger reactions. The initial reaction barrier of this one-step reaction profile lies between the *cis*- and *trans*-reaction profiles.

(4) A new reaction profile with concerted initial transition state (**conTS**) has been found for the Staudinger reaction of $PF_3 + N_3CH_3$. Rather than going through a more open PNNN-ring *cis*-intermediate (**cis**), this Staudinger reaction reaches a more closed PNNN-ring intermediate (**cisclose**) after the concerted initial transition state and then isomerizes to **cisopen** (similar to **cis**) intermediate.

(5) The reaction profile of the Staudinger reaction of $P(CH_3)_3 + N_3F$ in gas phase is different from that in a solvent, i.e., solvent effects can change the potential energy profile of this Staudinger reaction. The initial *trans*-transition state of the Staudinger reaction of $P(CH_3)_3 + N_3F$ disappears in DMSO. We found that adding electron-withdrawing groups to the azide and electron-donating groups to the phosphane can accelerate the Staudinger reaction in polar solvents.

Acknowledgment. The financial support from the Natural Sciences and Engineering Research Council (NSERC) of Canada is gratefully acknowledged. We thank Dr. Derek P. Gates for his initialization of and helpful discussions on this work. We also thank Prof. Grenfell N. Patey for his helpful comments on this work.

Supporting Information Available: Optimized Cartesian coordinates of all the structures at the level of B3LYP/6-31G(d) from Gaussian calculations and relevant molecular orbital diagrams of intermediates, **cis** and **trans**, in the Staudinger reactions. This material is available free of charge via the Internet at http://pubs.acs.org.

JO049702N